No.12 Journal of Petroleum Research & Studies

Performance and Sensitivity analysis of Factors Affecting NOx Emissions from Hydrogen Fueled SI Engines

Eiman Ali Eh. Sheet

Energy and Renewable Energies Technology Center, UOT.

Abstract

An Analysis of Variance (ANOVA) sensitivity analysis using suitable MATLAB code on the factors affecting oxides of Nitrogen (NOx) emissions of a hydrogen powered 4-stroke, water-cooled spark-ignition engine was conducted in this work. This was done using specialized engine performance and emission simulation software. The parameters studied were the engine speed, air-fuel equivalence ratio, spark plug location in addition to some other combustion parameters like combustion duration, heat loss besides some other useful performance parameters. It was found that NOx formation is minimum at peripheral spark location, slightly lean (PHI=0.9), and less advance timing is needed. Further, based on ANOVA analysis, the combination of engine speed and spark location has more significance (effect based on P-value) compared with engine speed and equivalence ratio. The combination of engine speed and ignition timing has more significance (effect based on P-value) compared with engine speed and equivalence ratio. Also found that NOx emissions behavior is more clear at lean mixture (PHI = 0.7), central spark location (XSP = 0.5) and retarded ignition timing (IGN near zero).

Keywords: Hydrogen fuel, ANOVA, Engine performance, Hydrogen combustion, Engine pollution.

Introduction

Several factors stimulated the search for alternative fuels to replace or supplement the conventional fuel used in Iraq. First and foremost was the environmental damage caused by the two major wars of 1990 and 2003. These wars drastically affected the ecosystem and caused major reduction in green areas which resulted in the degradation of the quality of ambient air. In addition to the above reasons, the combustion of high sulfur content gasoline and diesel in electrical generators and motor vehicles increased the concentrations of CO, NO2, SO2, and HCs in the atmosphere. These factors made it necessary for the authorities in Iraq to search for alternatives to the current sources of energy. This work deals with one of the most suitable, clean burning and renewable alternative i.e. Hydrogen.

The potential for hydrogen-fueled internal combustion engines (H_2ICEs) to operate as clean and efficient power plants for automobiles is now well-established and documented in the literature. In particular, H_2ICEs with near-zero emissions; and efficiencies in excess of conventional gasoline-fueled ICEs have been demonstrated (e.g. [1–2]).

The literature on the H_2ICE is voluminous. An excellent historical perspective of the hydrogen engine and technical review of H_2ICE research prior to 1990 can be found in Das [3].

Some of the key properties of hydrogen that are relevant to its employment as an engine fuel are discussed in [4]. Hydrogen has a wide flammable mixture range in air to permit extremely lean or rich mixtures support combustion. It burns faster and produces higher energy compared with gasoline Therefore, it can be said that the engine design has to be modified to suit the properties of the new fuel.

During World War I [5] hydrogen and pure oxygen were considered for submarine use because the crew could get drinkable water from the exhaust.

Hydrogen was also considered for use in powering airship engines. The gas used for buoyancy could also be used for fuel. Even if helium were used to provide lift, hydrogen gas could be used to supply additional buoyancy if stored at low pressure in a light container. It was Rudolf A. Erren who first made practical the hydrogen-fueled engine in the 1920s and converted over

1,000 engines. His projects included trucks and buses. After World War II the allies discovered a submarine converted by Erren to hydrogen power. Even the torpedoes were hydrogen powered.

In 1924 Ricardo conducted the first systematic engine performance tests on hydrogen. He used a one cylinder engine and tried various compression ratios. At a compression ratio of 7:1, the engine achieved a peak efficiency of 43%. At compression ratio of 9.9:1, Burnstall obtained an efficiency of 41.3% with an equivalency ratio range of 0.58-0.80.

Al-Baghdadi [6] also developed a theoretical model to study the performance of spark ignition (SI) engines using different alternative fuels including hydrogen. The mathematical and simulation model has been developed, tested, and verified against the experimental data to simulate a 4-stroke cycle of a spark ignition engine fueled with gasoline, ethanol, or hydrogen as a single fuel or their mixture. He reported that the model was capable to predict satisfactorily the performance and emissions including the incidence of pre-ignition at various engine-operating conditions. A good agreement was obtained between the results of the model and the experimental results were also reported.

Das *et.al.* [7] evaluated the potential of using a clean-burning fuel such as hydrogen for small horsepower spark ignition engines. He compared the performance of the engine using Hydrogen and Compression natural gas (CNG) fuels separately. They reported that the brake specific fuel consumption was reduced and the brake thermal efficiency improved with hydrogen operation compared to systems running on compressed natural gas. The brake thermal efficiency was as high as 31.19% for hydrogen operation compared to that of 27.59% for CNG.

Murat *et.al.* [8] studied experimentally the performance and emissions of a small engine with hydrogen at a suitable lean mixture without backfire. The main aim of the study is to test the improvement on the engine performance, fuel consumption and emissions. They reported reduction in both the specific fuel consumption and NOx emissions by about 57% and 66%, respectively using hydrogen as fuel. Moreover, the values near zero for CO, CO_2 and HC

emissions were also reported. They also reported no backfire occurrence for this small engine at certain suitable lean mixture.

Chuayboon *et.al.* [9] studied the performance four-stroke spark ignition gas engine operated on mixtures of CH_4, H_2 and CO_2. They conducted their experiments at a constant engine speed of 2,000 rpm and throttle opening of 14% with various equivalence ratios. They reported that the highest brake power output of 12.5 kW and 35% thermal efficiency were achieved when operated with the mixture of 69.70% CH_4, 9.95% H_2 and 20.45% CO_2 and the equivalence ratios between 1.0 and 0.82.

Kenji *et.al.* [10] studied the possibility of achieving large output power, compactness and lightness in weight, high thermal efficiency and near-zero emissions without any exhaust gas after-treatment using a small 3-cylinder, 4-stroke hydrogen fuelled direct injection engine converted from a gasoline direct injection engine with a 660 cc displacement and the compression ratio of 9.1. They reported that the NOx emission was independent of the intake air pressure, rather dependent on the air excess ratio expectedly, and that the maximum brake thermal efficiency was 34 % at the largest intake air pressure of 200 kPa. They attributed this to the leaner combustion which decreases the cooling loss.

Cheolwoong *et.al.* [11] studied the use of Hydrogen-compressed natural gas (HCNG) technology as a promising alternative to that used in conventional compressed natural gas engines on the engine performance and emission levels under variable valve overlap periods. They found that the torque valve could meet engine emission specifications, the hydrocarbon and methane emissions were reduced by approximately 41% by decreasing the valve overlap duration while using HCNG fuel. The level of NOx emissions was approximately equivalent to or slightly higher than that of a conventional camshaft.

Fanos *et.al.* [12] studied the effect of simultaneous H_2 + N_2 intake charge enrichment on the emissions and combustion of a compression ignition engine. Bottled H_2 + N_2 were simultaneously admitted into the intake pipe of the engine in 4% steps starting from 4% (2% H_2 + 2% N_2) up to 16% (v/v). The results showed that under specific operating conditions H_2 + N_2 enrichment can offer simultaneous NOx, BSN and CO emissions reduction.

Joachim *et.al.* [13] investigated the heat transfer mechanisms in a hydrogen engine by measuring the instantaneous heat loss inside a spark-ignition engine at three locations. They used the design of experiment concept in their test. They showed that the effect of the engine factors was similar for all the fuels. However, the heat loss to the cylinder walls of hydrogen was only at the same level of that of the other fuels for very lean mixtures. The engine efficiency drastically reduced for rich mixtures as a consequence, indicating that a lean mixture in combination with boosting and external gas recirculation should be used to obtain high power outputs with high efficiencies for port fuel injected engines.

Shivaprasad *et.al.* [14] experimentally investigated the performance and emission characteristics of a high speed single cylinder SI engine operating with different hydrogen gasoline blends. They modified the conventional carbureted engine with electronic fuel injection system. Their test results demonstrated that combustion performances, fuel consumption and brake mean effective pressure were eased with hydrogen enrichment. They experimental also showed that the brake thermal efficiency was higher than that for the pure gasoline operation. Moreover, HC and CO emissions were all reduced after hydrogen enrichment.

As noticed from the above researchers' work is that their main focus is on the engine performance and emissions using different technique. In addition to this, this research examines the sensitivity of each parameter on the final results by finding their effectiveness and degree of influence using the ANOVA technique.

The objective of this work was to investigate the effect of different engine speeds (1000 rpm to 3000 rpm), equivalence ratios from 0.7 to 1.2, wide open throttle (WOT), maximum brake torque angle (MBT) and compression ratio (CR) of 9.0 and on the Ricardo E6/T Variable Compression Ratio engine having the following specifications: single cylinder, 4-stroke, water-cooled, variable compression ratio spark ignition engine.

The study was conducted using specialized Engine Simulation Software.

Brief Description Of Simulation Model

The main program consists of two main stages: (1) The pipe calculations, and (2) the cylinder calculations. The cylinder calculations are further subdivided into two main stages: (1) power cycle and (2) gas exchange process. The power cycle is subdivided into three main stages: (1) compression, (2) ignition or combustion and (3) expansion or power stroke. Finally, the expansion stroke is further subdivided into (1) expansion with two zones (burned and unburned), and (2) expansion of full products. The model was modified with the inclusion of the gas exchange model, the turbulent combustion model, and the inclusion of the calculation of the friction parameters of various parts of the engine. Since describing the complete model would make this paper extremely lengthy and would bring it out of scope of the main topic, below is a brief description of the model.

Compression

The pressure and temperature in this stroke is calculated using the first law of thermodynamics equations and the equation of state as given in [15]:

$$\frac{dp}{d\theta} = \left\{ \frac{R}{C_v}\left(\frac{dQ}{d\theta}\right) - p\frac{dV}{d\theta}\left(\frac{R}{C_v}+1\right) \right\} / V \quad \ldots\ldots\ldots\ldots (1)$$

$$\frac{dT_u}{d\theta} = T_u\left(\frac{1}{V}.\frac{dV}{d\theta} + \frac{1}{p}.\frac{dp}{d\theta}\right) \quad \ldots\ldots\ldots\ldots\ldots (2)$$

$$\frac{dW}{d\theta} = p\frac{dV}{d\theta} \quad \ldots\ldots\ldots\ldots\ldots (3)$$

The heat transfer rate from the gas to wall is calculated using Annand's equation [16]:

$$\frac{Q}{A} = \frac{a\,k_q}{D}(R_e)^b(T_u - T_w) \quad \ldots\ldots\ldots\ldots\ldots\ldots (4)$$

where $K_q = \frac{C_p \mu}{0.7}$. The variables are continuously updated during calculation using the general formula:

$$x_{n+1} = x_n + \frac{dx}{d\theta}\Delta\theta \quad \text{.........................} \quad (5)$$

where "x" is any variable. The numerical procedure used for this purpose is the Runge-Kutta Method.

Ignition

The calculations then proceed in three phases. Firstly, the initiation of the combustion, then the subdivision of the combustion chamber into two zones separated by spherical flame front and, finally a single zone encompassing the whole of the combustion chamber. To initiate the combustion a unit mass of the cylinder content is considered to burn at constant volume. The internal energy of the initial reactants is set equal to the internal energy of the products. The first guessed value of the burnt temperature "T_b" is calculated using the Annand's equation [2] as below:

$$T_b = T_u + 2500 * \phi * X_f \qquad \text{for } \phi \le 1.0 \text{ ....} \ (6)$$

$$T_b = T_u + 2500 * \phi * X_f - 700 * (\phi - 1.0) * X_f \qquad \text{for } \phi > 1.0 \text{ ....} \ (7)$$

$$T_b = T_b - \delta T_b \text{ ....} (8)$$

where, $\delta T_b = (e_b - e_u) / C_{vb}$.

Further, the following turbulent flame speed equation for pure hydrogen given by [17] was used:

$$Ut = 5000 * \left[\frac{0.1 * N * D * S * P}{T_b^{1.67}}\right]^{0.4} * (T_b^{0.41} * T_u^{1.25}) * (Rmol / Ea) * \left[\frac{X_f\left(1 - \phi * \left(1 - \frac{Rmol * T_b^2}{Ea * (T_b - T_u)}\right)\right)}{\phi}\right]^{0.5} * \exp\left(\frac{-Ea}{2.0 * Rmol * T_b}\right)$$

……(9)

Species Formation

The governing equations for the mechanism of NO formation are given in [18,19, 20]:

$N+NO \Leftrightarrow N_2+O$ $K_{f1} = 3.1*10^{10} * e^{(-160/T)}$ $m^3/kmols$

$N+O_2 \Leftrightarrow NO+O$ $K_{f2} = 6.4*10^{6} * T * e^{(-3125/T)}$ $m^3/kmols$

$N+OH \Leftrightarrow NO+H$ $K_{f3} = 4.2*10^{10}$ $m^3/kmols$

$H+N_2O \Leftrightarrow N_2+OH$ $K_{f4} = 3.0*10^{10} * e^{(-5350/T)}$ $m^3/kmols$ …..10

$O+N_2O \Leftrightarrow N_2+O_2$ $K_{f5} = 3.2*10^{12} * e^{(-18900/T)}$ $m^3/kmols$

$O + N_2O \Leftrightarrow NO+NO$ $K_{f6} = K_{f5}$ $m^3/kmols$

$N_2O+M \Leftrightarrow N_2+O+M$ $K_{f7} = 10^{12} * e^{(-30500/T)}$ $m^3/kmols$

In these equations the rate constants (K_{fi}) are all in m^3/kmols. 'M' is a third body which may be involved in the reactions, but is assumed to be unchanged by the reactions. 'M' can be assumed to be N_2. These equations can be applied to the zone containing "burned" products, which exists after the passage of the flame through the unburned mixture. It will be assumed that H and OH, and O and O_2 are in equilibrium with each other; these values can be calculated by the methods given in [18].

Referring to equations (10) the net rate for NO can be derived as follows:

$$K_{f1}[N][NO]+K_{b1}[N_2][O] = - \alpha\beta K_{f1}[N]e[NO]e+K_{b1}[N_2]e\,[O]e \quad \ldots\ldots\ldots\ldots(11)$$

But,

$$K_{f1}\,[N]e\,[NO]e = K_{b1}\,[N_2]e\,[O]e = R_1$$

So the net rate from the first equation of the set of equations (10) becomes - $\alpha\ \beta\ R_1 + R_1$. Using similar procedure for the rest of equations of (10) involving NO, N_2O and finding R_2 through R_7 and using the following expressions

$$\beta = \frac{R_1 + \alpha(R_2 + R_3)}{(\alpha R_1 + R_2 + R_3)} \quad \text{and} \quad \gamma = \frac{R_4 + R_5 + \alpha^2 R_6 + R_7}{(R_4 + R_5 + R_6 + R_7)}$$

gives the following expression for the rate of formation of (NO) as :

$$\frac{1}{V}.\frac{d}{dt}[[NO].V] = 2.(1-\alpha^2)\left[\frac{R_1}{1+\alpha\dfrac{R_1}{R_2+R_3}} + \frac{R_6}{1+\dfrac{R_6}{R_4+R_5+R_7}}\right] \quad \ldots\ldots\ldots (12)$$

Analysis Of Variance (ANOVA)

Analysis of variance (ANOVA) tests the hypothesis that the means of two or more populations are equal. ANOVA assesses the importance of one or more factors by comparing the response variable means at the different factor levels. The null hypothesis states that all population means (factor level means) are equal while the alternative hypothesis states that at least one is different.

To perform an ANOVA, one must have a continuous response variable and at least one categorical factor with two or more levels. ANOVA require data from approximately normally distributed populations with equal variances between factor levels. However, ANOVA procedures work quite well even if the normality assumption has been violated, unless one or more of the distributions are highly skewed or if the variances are quite different. Transformations of the original dataset may correct these violations.

P-value

Used in hypothesis tests to help you decide whether to reject or fail to reject a null hypothesis. The p-value is the probability of obtaining a test statistic that is at least as extreme as the actual calculated value, if the null hypothesis is true. A commonly used cut-off value for the p-value is 0.05. For example, if the calculated p-value of a test statistic is less than 0.05, you reject the null hypothesis. The p-value for each effect is given by the following:

$$P = 2\,P\,(T \geq |t|) \quad \ldots\ldots\ldots\ldots\ldots\ldots\ldots \quad (13)$$

Where t is the observed t-value and T follows a t-distribution with $n_1 + n_2 - 2$ degrees of freedom.

T-value

Compare the t-value to the t-distribution to determine if a predictor is significant. The bigger the absolute value of the t-value, the more likely the predictor is significant. The t-value for each effect is given by the following:

$$t = \text{Effect} / \text{SE} \quad \ldots\ldots\ldots\ldots\ldots\ldots\ldots\ldots\ldots\ldots\ldots \quad (14)$$

$$t = r\sqrt{\frac{n-2}{1-r^2}} \quad \ldots\ldots\ldots\ldots\ldots\ldots\ldots\ldots\ldots\ldots\ldots\ldots\ldots \quad (15)$$

Where;

SE is the standard error for the effect

r is the observed value of the correlation coefficient

n is the number of observations for each response

Variance inflation factor (VIF)

Used to detect multicollinearity (correlated predictors). VIF measures how much the variance of an estimated regression coefficient increases if your predictors are correlated. Minitab calculates VIF by regressing each predictor on the remaining predictors and noting the R^2 value. For predictor x_1, the VIF is:

$$VIF = \frac{1}{1 - R^2(x_1)} \qquad \text{.....(16)}$$

Standard error of the difference

Minitab uses the following formula to calculate the standard error of the difference, SE:

$$SE = \frac{S}{\sqrt{n}} \qquad \text{..... (17)}$$

Where S is the standard deviation of the observations and n is the number of observations.

Model Modification and Verification

Before we proceed with the study, there was a need to verify the model for the case of Hydrogen-fueled engines. This was the first part of this study. For this part the thermodynamic, physical, chemical and coefficients of certain thermophysical properties of hydrogen were incorporated since the properties of fuels affect the performance of the engine. Some of the Hydrogen properties are shown below:

Hydrogen Fuel Data:

Internal Energy Coefficients for polynomial expression [18] where

$$e(T) = Rmol \left[\sum_{i=1}^{i=5} M_i \left[\left[\left[\sum_{j=1}^{j=5} a_{ij} T^j \right] - T \right] + \frac{h_{oi}}{R_{mol}} \right] \right] \qquad (18)$$

	3000 > T > 500 K	3000 >T > 6000 K
a_1	3.43328	3.21299
a_2	-8.18100e-06	2.87156e-04

a_3	9.66990e-08	-2.28839e-08
a_4	-1.44392e-11	7.66560e-13
a_5	0.0	0.0
ho	0.0	0.0

Viscosity Coefficient (kg/m.s): 8.6e-06

Calorific Value (kJ/kg): 119617

Annand's Constants:

a	0.40	
b	0.70	
c	0.4284e-011	(kW/m^2K^4)

The engine design and operating parameters are shown in table (1).

Table (1): Engine design parameters.

Engine speed	variable
Cylinder bore	76.2 mm
Stroke	111.125 mm
Connecting rod length	233.35 mm
Displacement volume	506 cm^3
Compression Ratio	variable
Intake valve data	
Diameter	35.0 mm
Opens	9^o bTDC
Closes	36^o aBDC
Exhaust valve data	
Diameter	30.05 mm
Opens	42^o bTDC
Closes	7^o aBDC
Ignition timing	variable

Then, the experimental data of the Ricardo E6/T variable compression ratio engine with CR of 7.5, equivalence ratio (ϕ) of 1.0 and maximum brake torque (MBT) spark timing were compared with the calculated data. The results of the mathematical model are shown in Figures (1-a and 1-b). Both figures show that simulation model was able to predict the performance of H_2-powered IC engine with good degree of accuracy. These errors in the mathematical model are mainly attributed to the engine design data that could not be

measured, age effect as well as the exact chemical composition of the exhaust and cylinder products.

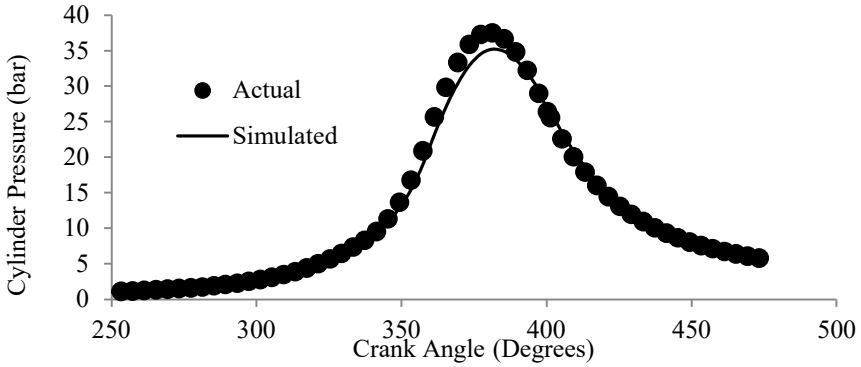

Fig.(1)-a: Cylinder pressure comparison between measured and model.

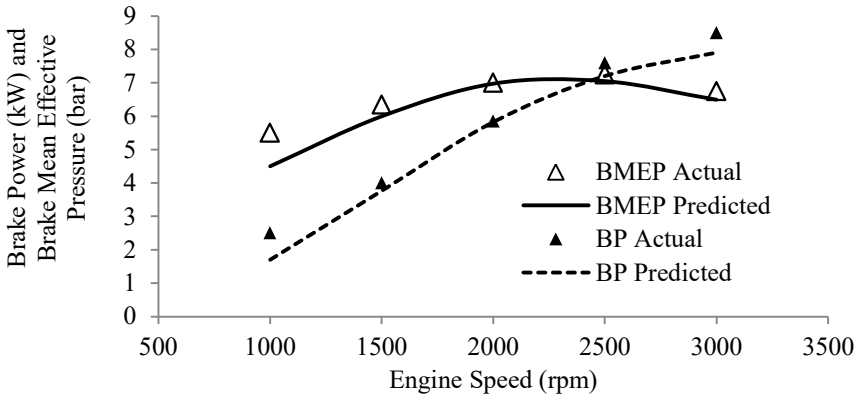

Fig.(1)-b Power and mean effective pressure comparison between the calculated and model.

Results and Discussion

In the following section the effect of engine speed, compression ratio, equivalence ratio, spark plug location and spark timing on the performance parameters like brake mean effective pressure (BMEP), brake specific fuel consumption (BSFC), brake thermal efficiency, heat losses, flame speed, combustion duration and nitric oxides (NOx) levels have been discussed using hydrogen as a fuel in spark ignition (SI) engines.

1. Effect of engine operating variables

Before proceeding with the discussion it would be appropriate to define the term spark plug location ratio "XSP" used in the program. With the help of

Figure (2), XSP can be understood to be a non-dimensional parameter referring to the ratio of the distance between the spark plug from the nearest wall (B) to the cylinder diameter (D) i.e. $XSP = \frac{B}{D}$. This has range from 0.0 at the peripheral to 0.5 at the center.

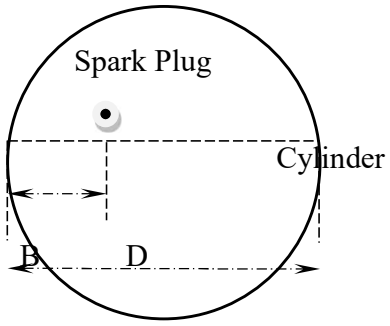

Fig.(2) Definition of spark plug location.

Figures (3- 5) show the effect of engine speed, spark plug location equivalence ratio and spark advance on the engine NOx emitted. It is noticed from figure (3) that for all engine

speeds the amount of NOx emitted increases as the spark advance angle (IGN) increases. This is because advancing the ignition timing causes the combustion process to occur earlier in the cycle which leads to increase peaks of pressure and temperature during the combustion process, since most of the fuel is burned before top dead center. Further, advancing the ignition timing makes the peak pressure to happen closer to top dead center where the cylinder volume is smaller and hence, makes the combustion occur near top dead center which is the ideal crank angle for combustion. Hence advancing the ignition timing leads to improve the engine thermal efficiency. Also, advancing the ignition timing also increases the residence time and the activity of partial oxidation reactions during the compression stroke.

On the other hand, retarding the ignition timing decreases the pressure and temperature peaks during the combustion process because there is not enough time between the ignition timing and top, dead center to complete the chemical reaction. Thus, large amounts of fuel burn after top dead center in the expansion stroke. This is in agreement to the findings of so many researchers e.g. [21, 22, and 23].

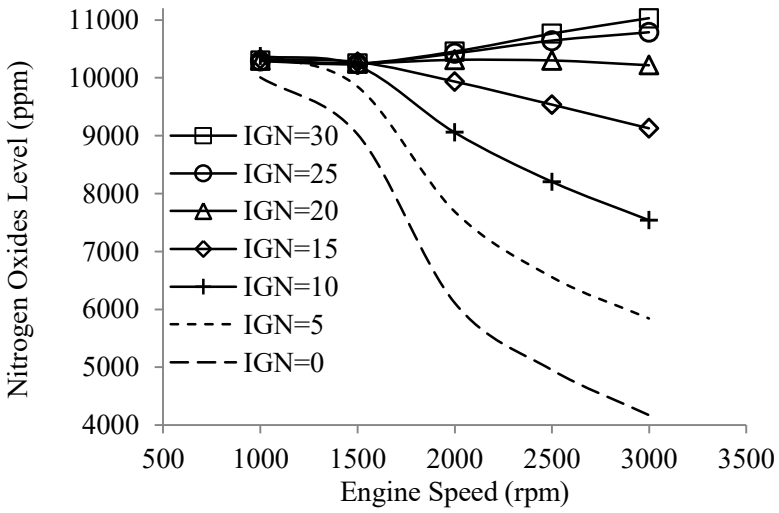

Fig.(3) Variation of NOx level with engine speed at different spark advance timing.

As seen from the kinetics model of NO formation (equations 10 and 12), the rate of NO formation is dependent on the temperature and Oxygen availability in addition to the exposure time.

Figure (4) clearly shows the effect of air-fuel equivalence ratio (Phi) on the NOx formation. This change in NOx level is more clear at lean mixtures (due to higher oxygen availability) and at lower speeds due to time and oxygen availability and less thermal losses in addition to the improved thermal efficiency.

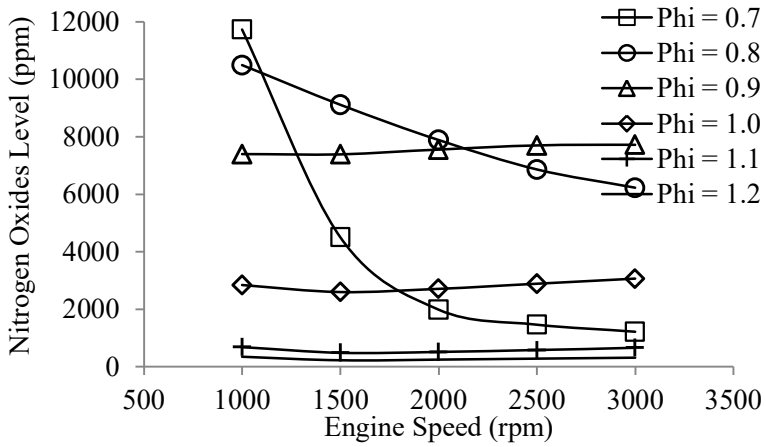

Fig. (4) Variation of NOx level with engine speed at different equivalence ratios.

In figure (5), the effect of spark plug location on the formation of NOx is shown. It is clear that as the spark is shifted near the center, the NOx formation becomes more rapid. This is due to the shortening of the time available by the products of combustion to lose its heat to the coolant. Further, central spark provides better combustion since the flame travel distance is halved and hence the combustion efficiency improves.

The above figures were further tested using ANOVA technique to check the most sensitive or influential factor or combination of factors that affect the NOx formation. This was necessary for further analysis. This is the first time that such sensitivity analysis is done on NOx formation using alternative fuel.

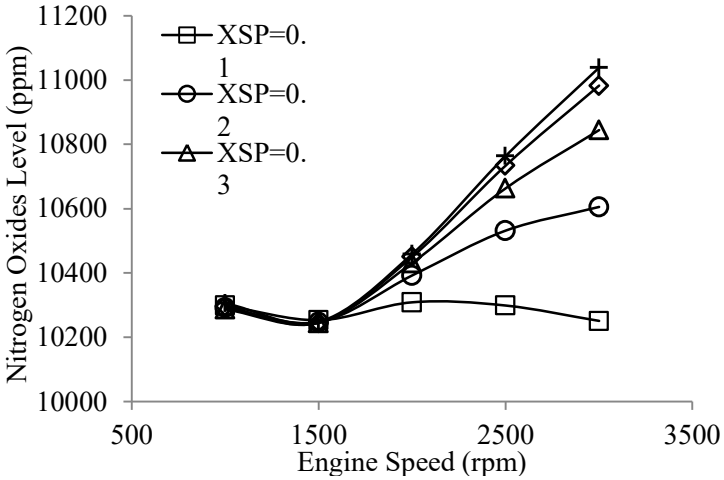

Fig.(5) Variation of NOx level with engine speed at different spark locations

Using MATLAB (ANOVA) routines with sight modifications, the three combinations i.e. engine speed; spark plug location ratio and equivalence ratio were tested and revealed the following results:

As for the combination between engine speed and spark plug location ratio, shown below, both factors are equally influential since they are also dependent on one another. This is shown by the P-value.

Term	Coef	SE Coef	T-Value	P-Value	VIF
Constant	9753	103	94.58	0.000	
Speed	0.2494	0.0397	6.28	0.000	1.00
XSP	690	198	3.48	0.002	1.00

Regression Equation NOx = 9753 + 0.2494 Speed + 690 XSP

The above ANOVA results clearly show that due to the lower P-value and higher VIF value, both variables i.e. engine speed as well as spark plug location ratio are significant and influential in NOx formation.

The other combination showed different results between engine speed and equivalence ratio. The results showed less dependent on engine speed if combined with equivalence ratio. This

proves the effect of Oxygen availability. Further, this is expected since there is no direct relation or effect between both variables.

Term	Coef	SE Coef	T-Value	P-Value	VIF
Constant	18839	3122	6.03	0.000	
Speed_1	-1.104	0.699	-1.58	0.126	1.00
PHI	-13382	2892	-4.63	0.000	1.00

Regression Equation NOx = 18839 - 1.104 Speed - 13382 PHI

The above ANOVA results clearly show that due to the higher P-value for engine speed, hence this variable is insignificant in NOx formation at different equivalence ratios.

The third combination between the engine speed and spark advance also was tested and revealed the results below. The results shows without any doubt the effect of ignition advance and engine speed combination.

Term	Coef	SE Coef	T-Value	P-Value	VIF
Constant	9512	618	15.39	0.000	
Ign	122.4	18.4	6.64	0.000	1.00
Speed	-1.021	0.261	-3.92	0.000	1.00

Regression Equation NOx = 9512 + 122.4 Ign - 1.021 Speed

The above ANOVA results clearly show that due to the lower P-value and higher VIF value, both variables i.e. engine speeds as well as ignition timing are significant and influential in NOx formation.

To realize this behavior of the engine let us look inside the engine and examine what is the effect of certain combustion factors on NOx formation.

The factors are many, hence, this study will concentrate on combustion-related factors like brake power, heat loss, combustion duration, thermal efficiency and peak cylinder burned temperature. The other design factor is the volumetric efficiency.

This study will be done at 20 degrees BTDC since it is the most stable angle (shows less variation in NOx with engine speed and SPL = 0.1 for it is the original location of the spark in the Ricardo Engine used.

2. Effect of brake thermal efficiency.

Thermal efficiency of an engine defines the fraction of heat that has been liberated by combustion that ends up in useful mechanical power output. Brake thermal efficiency compares the useful power available at the engine crankshaft (called brake power) with the energy actually supplied with the fuel.

It is calculated using the following equation:

$$\text{Brake Thermal Efficiency} = \frac{\text{Energy equivalent of brake power}}{\text{Energy input to the engine}} = \frac{\dot{W}_B}{\dot{m}_{f*}Q_{cv}} \quad \ldots\ldots\ldots (19)$$

where $\dot{m}_f$ is the amount of fuel consumed (kg/s) and Q_{cv} is the fuel calorific value (kJ/kg). this value is calculated during the simulation process.

Figure (6) shows the variation of brake thermal efficiency with NOx level at different air-fuel equivalence ratios.

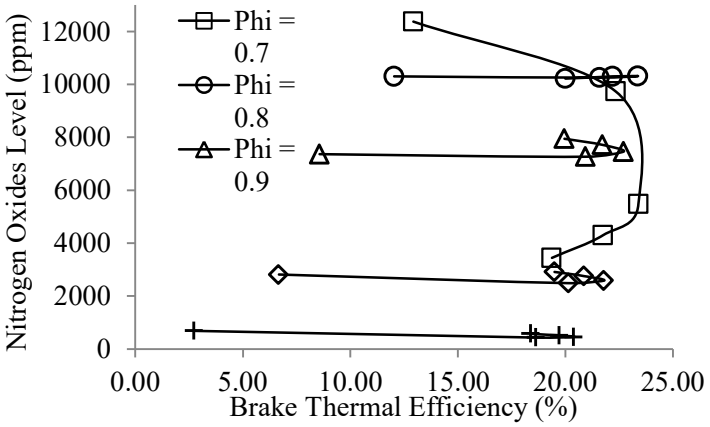

Fig.(6) Variation of NOx level with Brake Thermal Efficiency at different PHI

The figure shows inconsiderable variations in the NOx level except for PHI=0.7. Further, for all values of PHI, there is certain value of thermal efficiency for which the NOx level is maximum. Beyond this value the value of NOx decreases. This is expected to be due to the excess cylinder heat that might cause NOx to dissociate and increase in the heat loss to surrounding. This trend at PHI = 0.7 can be explained due to the higher thermal efficiency, combustion duration, oxygen availability and exposure time. This is because PHI = 0.7 means lean mixture, this in turn means higher amounts of air (or lees fuel) than the chemically correct (or stoichiometric) values. This is shown in figure (7).

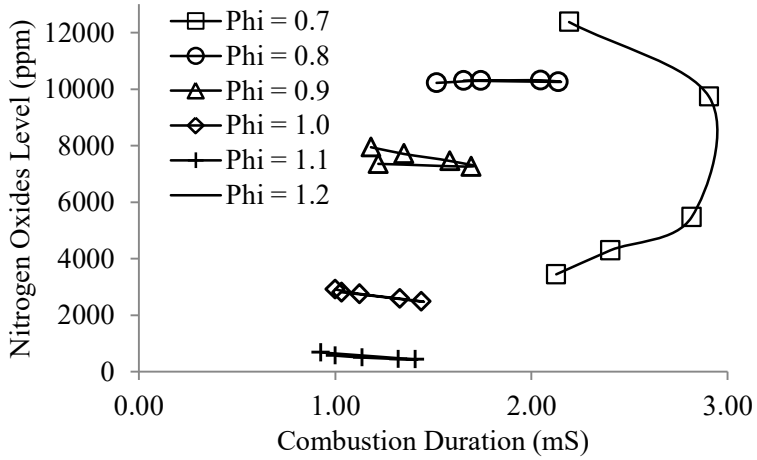

Fig.(7) Variation of NOx level with combustion duration at different PHI

3. Effect of Peak Cylinder temperature.

Cylinder temperature is an important factor affecting the kinetics of the NOx formation. There is an optimum value for which NOx has peak value. This is shown in figure (8).

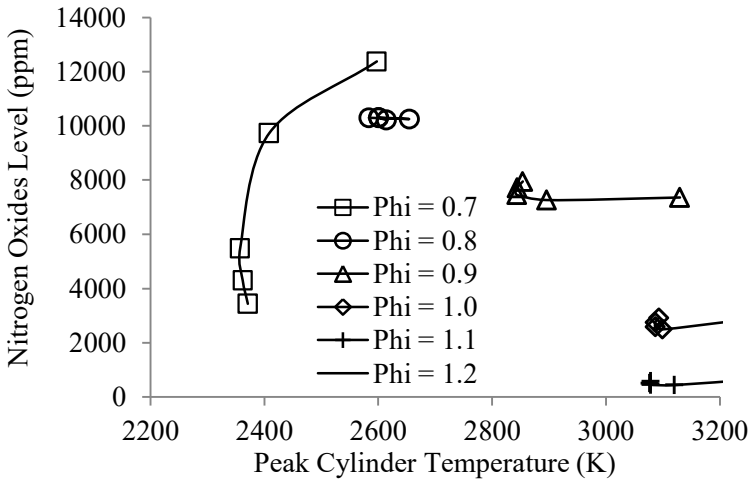

Fig.(8) Variation of NOx level with Peak Cylinder Temperature at different PHI

This is clear from the overall trend of the figure. Also noticed that the case of PHI=0.7 is the most affected case. This trend is understood with the help of figure (9) which shows a decrease in NOx emissions as the percentage heat loss is increased. Percentage heat loss is calculated by summing all the engine heat losses to coolant and exhaust and divided by the heat added due to combustion. Therefore, it gives the percentage heat lost with respect to the heat input to the engine.

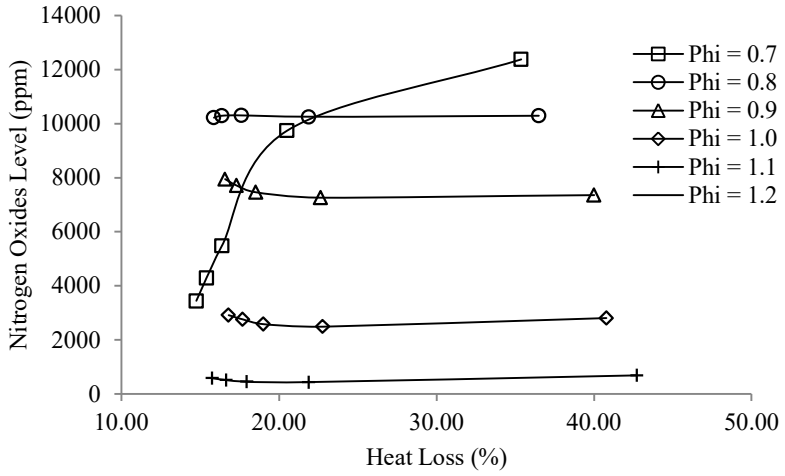

Fig.(9) Variation of NOx level with Heat Loss at different PHI

Another overall view of the figures reveals that at lean mixture (say PHI=0.7) due to the higher combustion durations, maximum thermal efficiency and cylinder temperature, the heat loss is increased as a result of higher temperature and hence the NOx formation is most varied.

Conclusion

According to the discussion of the obtained results, the following conclusions can be extracted:

1. Spark timing and location is found to have the strongest effect on NOx formation compared with engine speed and PHI.
2. To reduce the NOx formation, peripheral spark location, slightly lean (PHI=0.9), and less advance timing is needed.
3. The combination of engine speed and spark location has more significance (effect based on P-value) compared with engine speed and equivalence ratio.
4. The combination of engine speed and ignition timing has more significance (effect based on P-value) compared with engine speed and equivalence ratio.
5. Engine NOx emissions behavior is more clear at lean mixture (PHI = 0.7), central spark location (XSP = 0.5) and retarded ignition timing (IGN near zero).

Nomenclature

A = piston cross-section area, m^2

a = constant used in Annand's equation

b = constant used in Annand's equation

C_v = specific heat at constant volume, J/(kg K)

C_p = specific heat at constant pressuree, J/(kg K)

D = cylinder diameter, m

e = specific internal energy, J/(kg)

Ea = activation energy

K_q = thermal conductivity , W/(m K)

N = Engine speed, rev per minute

P = pressure,bar

Q = heat transfer rate, W

R = universal gas constant, J/(kg.K)

Rmol = gas constant , J/(kmol.K)

Re = Reynolds number , dimensionless

rpm = revolutions per minute

S = stroke length, m

T = absolute temperature, K

U_t = turbulent flame speed , m/s

V = cylinder volume, m^3

W = work, J

X_f = mole fraction of fresh mixture

Greek Symbols

θ = crank angle, deg.

μ = dynamic viscosity, kg/(m s)

ϕ = equivalence ratio, dimensionless

Subscripts

b burnt

u unburnt

w wall

References

1. Benson, R. S.: The Thermodynamics and Gas Dynamics of Internal Combustion Engine. Volume I, Clarendon press, Oxford (1982).
2. Gupta, H.N., Bansal, B.B., and Mohan, R.: Computer Simulation of Power Cycle for Spark-Ignition Engines. IE(I)-Journal-MC, 76, 130-133 (1995).
3. Das L. M.: Hydrogen engines: a view of the past and a look into the future. IJHE, 25, 581-589 (2000).
4. Karim, G.A.: Hydrogen as a spark ignition engine fuel. IJHE, 28, 569-577 (2003).
5. Erol Kahraman, Analysis of a hydrogen fueled internal combustion engine. A Thesis Submitted to the Graduate School of Engineering and Sciences of İzmir Instute of Technology in Partial Fulfillment of the Requirements for the Degree of MASTER OF SCIENCE in Energy Engineering, İZMİR, April (2005).
6. Maher A. R. S. A. "A Simulation Model for a Single Cylinder Four-Stroke Spark Ignition Engine Fueled with Alternative Fuels". Turkish J. Eng. Env. Sci. Vol. 30, PP. 331 – 350, (2006).
7. Das, L.M., Gulati R. and Gupta P.K., "A comparative evaluation of the performance characteristics of a spark ignition engine using hydrogen and compressed natural gas as alternative fuels". International Journal of Hydrogen Energy, 25, PP. 783-793, (2000).
8. Murat K., Bulent O. and Celik M. B., "The usage of hydrogen for improving emissions and fuel consumption in a small gasoline engine". J. of Thermal Science and Technology, 31, 2, 101-108, (2011).
9. Chuayboon, S., Prasertsan, S., Theppaya, T., Maliwan, K. and Prasertsan P. , "Effects of CH4, H2 and CO2 Mixtures on SI Gas Engine". Energy Procedia, 52, PP. 659 – 665, (2014).
10. Kenji N., Kimitaka Y. and Tetsuya O., "Potential of Large Output Power, High Thermal Efficiency, Near-zero NOx Emission, Supercharged, Lean-burn, Hydrogen-fuelled, Direct Injection Engines". Energy Procedia, 29, PP. 455 – 462, (2012).

11. Cheolwoong P., Sungwon L., Gihun L., Young C. and Changgi K. "Full load performance and emission characteristics of hydrogen-compressed natural gas engines with valve overlap Changes". Fuel, 123, PP. 101–106, (2014).
12. Fanos, C. and Athanasios, M., "Experimental investigation of the effects of simultaneous hydrogen and nitrogen addition on the emissions and combustion of a diesel engine". International journal of hydrogen energy, 39, PP. 2692-2702, (2014).
13. Joachim, D., Michel, D. P., Ivan, V. and Sebastian, V., "Heat loss comparison between hydrogen, methane, gasoline and methanol in a spark-ignition internal combustion engine". Energy Procedia, 29, PP. 138 – 146, (2012).
14. Shivaprasad, K. V., Raviteja, S., Parashuram C. and Kumar G. N., "Experimental Investigation of the Effect of Hydrogen Addition on Combustion Performance and Emissions Characteristics of a Spark Ignition High Speed Gasoline Engine". Procedia Technology, 14, PP. 141 – 148, (2014).
15. Yamin J. A.A. , "Comparative Study Using Hydrogen and Gasoline as fuels for 4-Stroke Spark Ignition Engines: Combustion Duration Effect", Accepted for publication in the International Journal for Engineering Research, (2006).
16. Annand, W. J. D., "Heat Transfer in the Cylinders of Reciprocating Internal Combustion Engines", Proc. Inst. Mech. Engrs. Vol. 177, No. 36, (1963).
17. Al-Janabi H.A.K.S, and Al-Baghdadi, M.A., "A prediction study of the effect of hydrogen blending on the performance and pollutants emission of a four stroke spark ignition engine". International Journal of Hydrogen Energy, 24 , pp. 363-375, (1999).
18. Winterbone, D. E.: Advanced Thermodynamics for Engineers. John Wiley & Sons, (1997).
19. Zareei, J. and Kakaee, A. H. : Study and the effects of ignition timing on gasoline engine performance and emissions. Eur. Transp. Res. Rev. 5:109–116 (2013)
20. Heywood, J., Higgins, J., Watts, P. and Tabaczynski, R.: Development and use of a cycle simulation to predict SI engine efficiency and NOx emissions. SAE Paper 790291 (1979).

21. Yang, J., and Jay K. M.: Predictions of the effects of high temperature walls, combustion, and knock on heat transfer in engine-type flows. SAE Paper 900690 (1990).
22. Farhad, S., Amir H. S. and Ali M. P.: NOx Control Using Variable Exhaust Valve Timing and Duration. SAE Paper 2009-01-1424 (2010).
23. Yamin J. A. A., Gupta, H. N., Bansal, B. B., and Srivastava, O. N.: Effect of combustion duration on the performance and emission characteristics of a spark ignition engine using hydrogen as a fuel. IJHE, 25, 6, 581-589 (2000).